



# Machine Learning Identifies Negative Emotions Encoded in the Cerebellum

Yitong Zhang<sup>1</sup> , Chenxuan Wu<sup>1</sup>, Beiyang Lin<sup>2</sup>, Yongyi Dou<sup>1</sup>, Lizhi Cao<sup>1</sup>, Hao Wei<sup>2</sup>, and Tianyi Yan<sup>1</sup> 

<sup>1</sup> Beijing Institute of Technology, Beijing 100081, China  
yantianyi@bit.edu.cn

<sup>2</sup> Beijing University of Posts and Telecommunications, Beijing 100876, China

**Abstract.** This study investigates the cerebellum's role in processing stress-induced negative emotions by analyzing neurophysiological signals from the deep cerebellar nuclei (DCN) in mice. We compared signals during chronic restraint stress and the tail suspension test, using implanted microwire electrodes to collect data from various DCN subnuclei, with a focus on the dentate and interstitial nuclei. Seventeen machine learning classifiers were employed to identify emotion encoding within low-frequency (0.5-49Hz) local field potentials (LFPs) in the cerebellar dentate nucleus. Notably, Medium Gaussian SVM, Medium Neural Network, Wide Neural Network, and Bilayered Neural Network demonstrated high accuracy in classifying emotional states via the cerebellar dentate nucleus, interstitial nucleus, and DCN. Our work proposes four classifiers suitable for distinguishing cerebellar negative emotion valence and provides evidence for the cerebellum's role in emotion encoding from a machine learning perspective. This research offers new insights into the neural circuitry mechanisms of depression and theoretical support for developing novel neuromodulation paradigms to treat depression.

**Keywords:** machine learning · local field potential (LFP) · power spectra

## 1 Introduction

The cerebellum is a crucial component of the motor system and is increasingly recognized for its involvement in non-motor behaviors [1]. Evidence indicates that the cerebellum significantly contributes to cognitive and emotional processes [2, 3]. A thorough comprehension of the neuronal coding in the cerebellum must encompass these non-motor functions. Processing of the brain's EEG signal data based on machine learning can identify anxiety and depression through classifier algorithms [4]. The analysis of cerebellar electrical signals holds a wealth of physiological and disease-related information. In clinical medicine, these signals serve as a diagnostic basis for certain brain diseases [5]. Moreover, in biological research, machine learning algorithms are utilized to identify EEG signals, enabling further analysis and investigation. Currently, depression diagnosis primarily relies on oral communication and questionnaire surveys,

which introduce uncertainties and are influenced by numerous factors, compromising the accuracy of results. Therefore, employing machine learning algorithms to analyze EEG signals offers a more precise and efficient approach for diagnosing depression. Remarkably, the recognition of depression using machine learning techniques achieves high accuracy rates, with the best accuracy reaching 90% [6]. However, due to the extensive involvement of the cognitive cerebral cortex in regulating depressive emotions, further research is needed to elucidate the complete relationship.

However, current research predominantly concentrates on analyzing EEG data from the cerebrum [7], neglecting the potential insights that could be gained from studying the cerebellum. The cerebellum is traditionally recognized for its role in maintaining motor balance and enhancing muscle tension. While limited research exists on its involvement in emotion regulation, relevant studies indicate that the cerebellum does play a role in emotion processing and regulation [8]. Furthermore, the cerebellum is a crucial component of the hypothalamus-cerebellum-amygdala neural circuit involved in exercise-induced anxiety relief. This circuit, with the cerebellum at its core, facilitates anxiety reduction and other symptom alleviation through physical activity [9]. In a study [10], electrical stimulation revealed significant changes in the number of c-Fos cells within the dentate nucleus, fastening nucleus of the cerebellum, and vestibular nucleus of the spinal cord in stressed animals. These findings suggest that the cerebellum may serve as an intermediate step in transmitting or mediating antidepressant behavior. Thus, it is plausible to conclude that the cerebellum plays a role in regulating depressive emotions. By considering these research findings, we can begin to appreciate the potential involvement of the cerebellum in emotional processes and its relevance to conditions like depression. Further investigation is warranted to fully understand the intricate mechanisms underlying the cerebellum's impact on emotional regulation and its implications for clinical interventions. Furthermore, while cortical EEG channels provide positional information, there is a dearth of empirical evidence regarding the discharge patterns of deep nuclei.

It is important to note that stress plays a significant role in the development of depression [11]. This study will utilize implanted microwire electrodes to gather data from various subnuclei within the deep cerebellar nuclei of healthy mice during both resting and stressful conditions, specifically focusing on the dentate nucleus (DN) and interstitial nucleus (IpN). The neuronal electrophysiological signals of these nuclei, as well as the encoding mechanisms of depressive emotions within the deep cerebellar nuclei, will be investigated using various machine learning algorithms.

It is commonly acknowledged that neurons transmit information through sequences of action potentials. Current neuro electrophysiological research predominantly concentrates on the action potentials of neurons, called spikes, thereby addressing only a portion of the coding mechanism of cerebellar neurons and overlooking the neural coding information conveyed by low-frequency signals. Oscillations ranging from 4–25 Hz have been observed in the granule cell layer of the primate parabolule and in rodents, with similar patterns recorded as local field potential (LFP) oscillations in the cerebellar cortex [12]. The theta rhythm represents a common neural activity that plays a crucial role in facilitating neural communication and synaptic plasticity within the brain. Through the concurrent recording of LFP signals in the medial prefrontal cortex (mPFC) and

cerebellum of TEBC guinea pigs, it was observed that theta frequency (5.0–12.0 Hz) oscillations in both regions became highly synchronized following the presentation of auditory conditioned stimuli [13]. In neuronal electrophysiology, low-frequency neural activity may serve as a potential form of neural coding. Due to the non-obvious nature of low-frequency signals, traditional methods struggle to elucidate pertinent biological principles. The advent of artificial intelligence presents an opportunity to address these challenges through machine learning techniques.

The remainder of this paper is organized as follows. The LFP recording and data preprocessing are presented in Sect. 2. Section 3 illustrated the Optimized Welch method for drawing power spectra. The power spectra of DN, IpN, and DCN is analysed by machine learning in Sect. 4 and Sect. 5, including algorithm performance analysis. Corresponding discussions are presented in Sect. 6, and Sect. 7 concludes the paper.

## 2 Local Field Potential Recording and Data Preprocessing

A 16-channel microwire electrode was surgically implanted into the mouse dorsal cochlear nucleus (DCN), allowing for simultaneous collection of local field potentials from all 16 channels. To ensure that emotional and movement information were not confounded in the emotion detection process, a behavioral paradigm involving chronic restraint and tail suspension tests was employed on healthy mice, inducing depressive-like emotions while varying the specific actions performed. The aim of this study is to investigate the neural coding characteristics of stress-induced negative emotions in the cerebellum by analyzing the similarities in two distinct actions. The experimental methodology involves the collection of EEG data, starting with a 10-min resting-state EEG recording, followed by EEG data collection of mice DCN under two different stress conditions. The experimental mice were categorized into DN ( $N = 18$ ) and IpN ( $N = 11$ ) groups based on the placement of microwire electrodes, both of which are classified as DCN sub-nuclei.

The EEG data collected underwent filtering using the Butterworth filter in the Offline Sorter software, with non-biological signals exhibiting high amplitudes in the time domain waveform being eliminated. During the tail suspension test, only the recorded signal during periods when the mouse was suspended and stationary was analyzed to mitigate the impact of movement interference. Following data processing, a total of 144 channels of CRS/resting state and TST/resting state were collected for subsequent analysis in the DN group, while in the IpN group, 80 channels of CRS/resting state and 96 channels of TST/resting state were collected for subsequent analysis.

## 3 Optimized Welch Method for Drawing Power Spectra

The average power of a power limited signal  $f(t)$  at time  $t \in [-T/2, T/2]$  can be expressed as formula (1).

$$P = \frac{1}{T} \int_{-T/2}^{T/2} f^2(t) dt \quad (1)$$

If signal  $f(t)$  can be identified with  $f_T(t)$  on time period  $t \in [-T/2, T/2]$ , and the Fourier transform of  $f_T(t)$  is  $F_T(\omega) = F[f_T(t)]$ , where  $F$  represents the Fourier transform. As  $T$  increases, the energy of  $F_T(\omega)$  and  $|F_T(\omega)|^2$  increases. When  $T \rightarrow \infty$ ,  $f_T(t) \rightarrow f(t)$ , and  $\frac{|F_T(\omega)|^2}{2\pi T}$  is approaching a limit. If this limit exists, its average power can be expressed in the frequency domain as formula (2).

$$P = \lim_{T \rightarrow \infty} \frac{1}{T} \int_{-T/2}^{T/2} f^2(t) dt = \int_{-\infty}^{\infty} \lim_{T \rightarrow \infty} \frac{|F_T(\omega)|^2}{2\pi T} d\omega \quad (2)$$

Define  $\frac{|F_T(\omega)|^2}{2\pi T}$  as the power density function of  $f(t)$ , also known as the power spectrum, expressed as formula (3).

$$P(\omega) = \lim_{T \rightarrow \infty} \frac{|F_T(\omega)|^2}{2\pi T} \quad (3)$$

The Welch average periodogram method involves segmenting the finite-length sequence  $x(n)$  of  $N$  points and averaging the periodogram. The input parameters for the Welch function include the Fourier series (fs),  $n$ -point fast Fourier transform (nfft), and noverlap. Noverlap, also referred to as the segment overlap coefficient, represents the degree of signal overlap and is measured in points. It can assume any value up to the number of nfft points, typically ranging from 20 to 50 percent of the total nfft points. The number of nfft points is determined by the sampling frequency and frequency resolution, which can be adjusted by changing the nfft value. The window function, denoted as window, should be shorter than the nfft points. A hamming window with a length equal to half the signal length was chosen for this study. Noverlap represents the number of overlapping sampling points in the segmented sequence, and its length should be less than the window function. By specifying the parameter noverlap, the segments could potentially overlap post-segmentation, thereby reducing variance. A value of 0.33 times the length of the window function was selected.

The power spectrum was calculated using the pwelch method, and the signal power spectrum with suitable resolution and smooth curve was obtained by averaging values at intervals of several points. The sampling frequency and sampling time were initially considered, with nfft points selected as 80000000, resulting in a power spectrum frequency resolution of 0.0005 Hz. In the analysis of the power spectrum, frequency and power averages are computed every 200 data points, resulting in a final frequency resolution of 0.1.

To enhance the clarity of distinguishing between two power spectrum curves, this study investigates two methods for reducing the frequency resolution of a signal segment to 0.1 Hz: (1) Decreasing the number of nfft points to reduce the resolution of the power spectrum (see Fig. 1a), and (2) Computing average values for specific intervals in the power spectrum diagram (see Fig. 1b).

## 4 Model Training Results and Test Analysis

During the feature extraction process, the Welch method was initially employed in Chapter 3, along with averaging at intervals of 200 frequency points, to derive the power spectrum. Subsequently, 485 power points ranging from 0.5 Hz to 49 Hz, with an

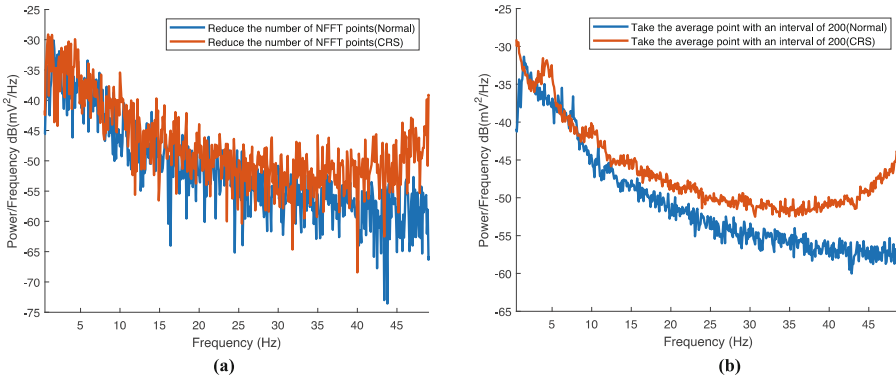


**Fig. 1.** Modify the number of nfft points (a) and reduce the frequency resolution comparison by averaging at intervals (b).

interval of 0.1 Hz, were selected as features. These features were then inputted into the classification learner tool in MATLAB, where all models were trained individually and validated using the 5-fold cross-validation method.

The neural coding mechanism for stress-induced negative emotions in the cerebellar dentate nucleus remains poorly understood, particularly with regards to the absence of a coding mechanism for low-frequency signals. This study aims to present evidence supporting the notion that low-frequency electrophysiological signals in the dentate nucleus encode negative emotions through the utilization of classification algorithms in the field of machine learning. Initially, the mouse EEG signal data obtained from the dentate nucleus was segregated into two groups: a control group consisting of resting state data collected prior to exposure to stressors, and a stress group representing the onset of stress-induced negative emotions. Data collected from various forced movements were randomly divided into a test set ( $N = 7$ ,  $n = 442$ ) and a training set ( $N = 2$ ,  $n = 128$ ) based on status;  $N$  denotes the quantity of animals providing input data, while  $n$  signifies the quantity of functional channels acquired by the multi-channel microwire electrode subsequent to preprocessing. Data of DN were analyzed using 17 algorithms across three categories (SVM, KNN, and neural network) as outlined in Table 1. Model performance was assessed through calculations of Accuracy, Precision, Recall, and AUC (ROC curve area).

The top 50% algorithms were selected based on three indicators: Accuracy, Precision, and Recall, as well as those with an AUC greater than 0.85. Upon comparing the performance of these algorithms across the 4 indicators, it was determined that the Medium Gaussian SVM, Medium Neural Network, Wide Neural Network, and Bi-layered Neural Network algorithms exhibited the most balanced performance (see Fig. 2).

Accuracy, the proportion of correctly identified true positive examples (TP) and true negative examples (TN) to the total identified samples, as formula (4).

$$\text{Accuracy} = \frac{\text{TP} + \text{TN}}{\text{TP} + \text{TN} + \text{FP} + \text{FN}} \quad (4)$$

**Table 1.** The model performance of the algorithms in classifying DN emotional encoding.

Machine learning models	Accuracy	Precision	Recall	AUC
Linear SVM	75.80%	67.40%	100.00%	0.89
Quadratic SVM	73.40%	65.60%	98.40%	0.99
Cubic SVM	79.90%	72.10%	96.90%	0.97
Fine Gaussian SVM	50.00%	50.00%	0.00%	0.89
Medium Gaussian SVM	85.90%	80.30%	95.30%	0.98
Coarse Gaussian SVM	71.90%	64.30%	98.40%	0.76
Fine KNN	57.00%	59.20%	45.30%	0.57
Medium KNN	69.50%	83.80%	48.40%	0.73
Coarse KNN	78.10%	80.00%	75.00%	0.81
Cosine KNN	71.10%	74.50%	64.10%	0.81
Cubic KNN	70.30%	88.20%	46.90%	0.76
Weighted KNN	68.00%	74.50%	54.70%	0.73
Narrow Neural Network	86.70%	88.50%	84.40%	0.93
Medium Neural Network	84.40%	78.90%	93.80%	0.95
Wide Neural Network	85.90%	78.80%	98.40%	0.94
Bilayered Neural Network	89.90%	89.20%	90.60%	0.94
Trilayered Neural Network	78.10%	75.70%	82.80%	0.83

**Table 2.** Classification accuracy for negative emotional encoding among cerebellum nuclei.

Machine learning models	DN	IpN	DCN
Medium Gaussian SVM	85.90%	81.20%	79.10%
Medium Neural Network	84.40%	84.40%	79.10%
Wide Neural Network	85.90%	62.50%	75.20%
Bilayered Neural Network	89.90%	67.20%	74.40%

Precision, the proportion of true positive examples (TP) to the predicted positive examples. Among them, the predicted positive example is equal to the correctly predicted positive example (TP) plus the incorrectly predicted positive example (FP), as formula (5).

$$\text{Precision} = \frac{\text{TP}}{\text{TP} + \text{FP}} \quad (5)$$

Recall, the proportion of true positive examples (TP) to the total actual positive examples. Among them, the total actual positive examples are equal to the correctly

predicted positive examples (TP) plus the incorrectly predicted negative examples (FN), as formula (6).

$$\text{Recall} = \frac{\text{TP}}{\text{TP} + \text{FN}} \tag{6}$$

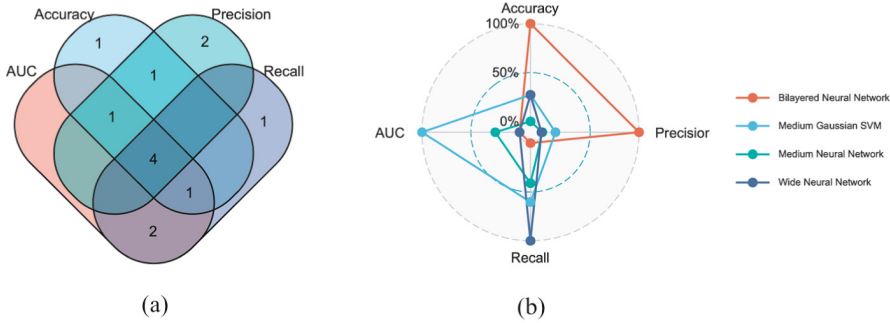
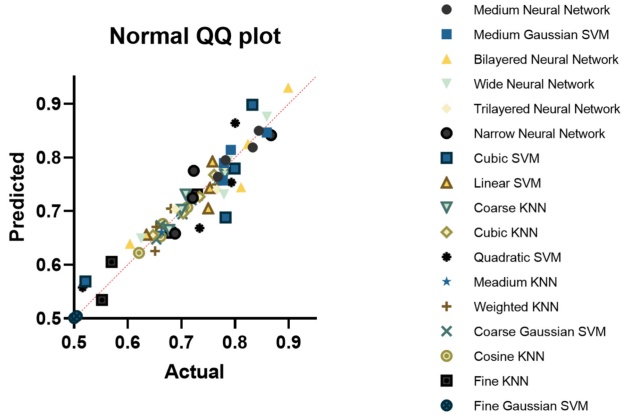


**Fig. 2.** The Venn diagram compares the superior algorithms among the four indicators (a), and the radar chart shows the balanced performance of the four algorithms (b).

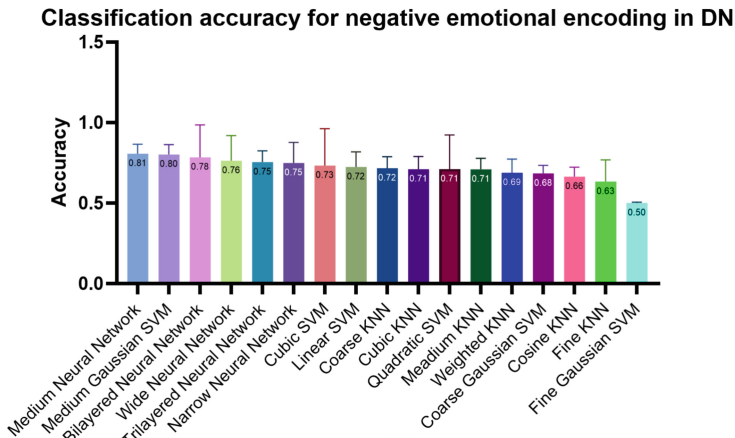
The aforementioned analysis findings indicate that the four algorithms exhibit optimal balanced performance, with less emphasis on classification accuracy. The objective of the machine learning exercise is to discern the involvement of low-frequency signals in the encoding of negative emotions within the cerebellar dentate nucleus, necessitating comparable accuracy in both non-interactive training and test datasets to support neurobiological investigations. Consequently, the dentate nucleus data was randomly divided three times, each subjected to individual machine learning analyses to determine the most effective algorithm for discerning negative emotion encoding. The evaluation was based on the average value and accuracy rate presented in Table 1, with the results summarized in Fig. 3. The Medium Gaussian SVM, Medium Neural Network, Wide Neural Network, and Bilayered Neural Network algorithms exhibited the highest accuracy rates, aligning with their selection as the top performers in terms of balanced performance.

### 5 Performance Analysis in Different Cerebellum Nuclei

The dentate nucleus is frequently cited as cerebellar nucleus involved in encoding negative emotions, however, further investigation is warranted into the coding role of the adjacent IpN and the DCN, including DN and IpN, in this process. Given the ability of four machine learning algorithms to effectively differentiate negative emotions encoded by the DN, we aim to apply these algorithms to EEG signal data collected from the IpN and the combination of IpN and DN to further elucidate their encoding capabilities. By analyzing the data obtained from the core and interpreting it in anatomical terms, we can assess the pivotal role of the algorithm in distinguishing depressive-like emotions in the cerebellum. This analysis also provides support for the theory that the cerebellar IpN is involved in encoding negative emotions.



(a)



(b)

**Fig. 3.** Normal QQ plot showed that, except for Medium Gaussian SVM, Trilayered Neural Network, Linear SVM, and Fine Gaussian SVM, all other classification algorithms obtained four accuracy values that conform to Gaussian distribution, Shapiro-Wilk test (a), and bar plot showed the average accuracy of classification models with 95% confidence interval (b).

The results presented in Table 2 demonstrate the classification accuracy of four different classifier algorithms for DN, IpN, and DCN. It was observed that the highest accuracy was achieved by the four algorithms in DN, with Medium Gaussian SVM and Medium Neural Network also performing well in IpN. Specifically, Medium Gaussian SVM and Medium Neural Network achieved accuracy rates of 81.20% and 84.40% respectively. However, Wide Neural Network and Bilayered Neural Network exhibited lower classification accuracy rates of 62.50% and 67.20% for negative emotion encoding in IpN. The classification accuracy for DCN ranged from 74% to 80%, indicating average performance across the four algorithms; this result may be related to the fact that the four algorithms are not suitable for IpN data.

## 6 Discussion

To control the frequency resolution in waveform analysis, it is common to adjust the parameters of the pwelch function, particularly by reducing the number of nfft points. However, this approach can lead to a sudden decrease in power values at various frequency points, resulting in sharp downward valleys in the power spectrum. These valleys, caused by the inherent randomness of bioelectric signals, not only hinder visual interpretation of the waveform but can also be erroneously identified as significant features by machine learning algorithms, thus impacting their effectiveness. This study improves the method of drawing the power spectrum. Compared with the power spectrum obtained by taking the average value at intervals of several points, the jitter amplitude of the curve is significantly reduced, and individual points do not appear. When the power suddenly increases or decreases, while retaining higher frequency resolution and not changing the spectrum information, the overall curve can become smoother, which greatly improves the effect of visually observing the power spectrum curve and allows for intuitive comparison. The difference between the power spectrum curves of normal state and pressure stress state. At the same time, using the power spectrum obtained by this method can avoid valleys in the power spectrum that affect the accuracy of machine learning. Investigating the neuroelectrophysiological properties of the cerebellar nuclei during stressful conditions can shed light on the neural circuit mechanisms underlying emotion regulation in normal physiological states.

Cerebellar neurons are involved in encoding negative emotions. In the context of local field potential analysis, which often focuses on time domain waveforms, we propose a novel approach to enhance estimation precision and accuracy. By dividing the long signal into multiple short segments based on the power spectrum obtained through the Welch method, performing FFT transformation on each segment, and subsequently averaging them, we observe significant improvements compared to the basic method. Typically, the spectrum of the corresponding time domain signal is used to reflect time-frequency changes in signal energy for most local potential studies [14]. In contrast, our approach transforms EEG waves, which exhibit amplitude changes over time, into the spectrum of EEG power varying with frequency. This enables intuitive observation of the distribution and changes in EEG rhythms.

In a recent study [15], the network connection from cerebellar crus I to the midbrain ventral tegmental area was elucidated through circuit mapping using adeno-associated virus and electrophysiological recording. This connection confirms the regulatory mechanism of the cerebellum on depression, specifically through the dentate nucleus of the deep cerebellar nucleus. In our work, we employ machine learning algorithms to identify that low-frequency electrophysiological signals in the dentate nucleus encode negative emotions. This finding further supports the role of the cerebellum in processing negative emotions and highlights the significance of low-frequency signals.

To study the cerebellum's involvement in depression, various methods have been employed, including the observation of c-fos expression in the cerebellum [16] and the analysis of structural magnetic resonance imaging data [17]. While the examination of action potentials and the generation of spikes are commonly used in neurological research to analyze neural activity, our study innovatively focuses on low-frequency neural signals. By comparing the encoding capabilities of different cerebellar nuclei, we

conclude that specific cerebellar nuclei encode depression, providing further evidence of the cerebellum's regulatory role. This emphasis on low-frequency neural activity as a potential form of neural coding strengthens our understanding of the neural mechanisms underlying depression.

In summary, our research sheds light on the involvement of cerebellar neurons in encoding negative emotions. By introducing a novel approach to local field potential analysis, we enhance estimation precision and accuracy. Through machine learning algorithms, we demonstrate the encoding of negative emotions in low-frequency electrophysiological signals within the cerebellum. These findings, combined with previous studies on c-fos expression and structural imaging, contribute to a comprehensive understanding of the cerebellum's regulatory role in depression, particularly with regard to low-frequency neural coding.

## 7 Conclusion

This study introduces four machine learning classifier algorithms that are adept at detecting negative emotion encoding within low-frequency signals of local field potentials in the rodent cerebellar dentate nucleus. Utilizing machine learning techniques, we aim to offer empirical support and suggest avenues for further research on the cerebellum's role in encoding negative emotions. Further exploration of DCN may elucidate its contribution to symptom manifestation in different disease states and offer potential opportunities for therapeutic interventions.

**Funding.** The authors declare financial support was received for the research, authorship, and publication of this article. This work was supported by the National Natural Science Foundation of China to Yitong Zhang (Grant Nos. 82302341).

## References

1. Washburn, Samantha, et al.: The cerebellum directly modulates the substantia nigra dopaminergic activity. *Nat Neurosci.* 27(3):497–513 (2024). <https://doi.org/10.1038/s41593-023-01560-9>. Epub 2024 Jan 25
2. Frazier M. R., et al.: A missing link in affect regulation: the cerebellum. *Social Cognitive and Affective Neuroscience* 17(12): 1068–1081(2022). <https://doi.org/10.1093/scan/nsac042>
3. Heck, Detlef H., et al.: The neuronal code (s) of the cerebellum. *J Neurosci.* 33.45: 17603–17609 (2013). <https://doi.org/10.1523/JNEUROSCI.2759-13.2013>
4. Hosseini M. P., et al.: A review on machine learning for EEG signal processing in bioengineering. *IEEE reviews in biomedical engineering* 14: 204–218(2020). <https://doi.org/10.1109/RBME.2020.2969915>. Epub 2021 Jan 22
5. Gavaret, M., Iftimovici, A., Pruvost-Robieux, E.: EEG: Current relevance and promising quantitative analyses. *Rev Neurol (Paris)*. 179(4), 352–360 (2023). <https://doi.org/10.1016/j.neurol.2022.12.008>. Epub 2023 Mar 10
6. Yasin, S., Othmani, A., Raza, I., et al.: Machine learning based approaches for clinical and non-clinical depression recognition and depression relapse prediction using audiovisual and EEG modalities: A comprehensive review. *Comput Biol Med.* 2023 Jun;159:106741. <https://doi.org/10.1016/j.compbiomed.2023.106741>. Epub 2023 Mar 4

7. Kamble, N., Shukla, D., Bhat, D.: Peripheral Nerve Injuries: Electrophysiology for the Neurosurgeon. *Neurol India*. 2019 Nov-Dec;67(6):1419–1422. <https://doi.org/10.4103/0028-3886.273626>
8. Batsikadze, G., Diekmann, N., Ernst, T.M., et al.: The cerebellum contributes to context-effects during fear extinction learning: A 7T fMRI study. *Neuroimage*. 2022 Jun;253:119080. <https://doi.org/10.1016/j.neuroimage.2022.119080>. Epub 2022 Mar 9
9. Zhang, X.Y., Wu, W.X., Shen, L.P., et al.: A role for the cerebellum in motor-triggered alleviation of anxiety. *Neuron*. 2024 Apr 3;112(7):1165–1181.e8. <https://doi.org/10.1016/j.neuron.2024.01.007>. Epub 2024 Jan 31
10. Wei, M.T., Wang, Q.Y., Jiang, X., et al.: Directed Connectivity Analysis of the Brain Network in Mathematically Gifted Adolescents. *Comput. Intell. Neurosci*. **28**(2020), 4209321 (2020). <https://doi.org/10.1155/2020/4209321>
11. Lebel, C., MacKinnon, A., Bagshawe, M., et al.: Elevated depression and anxiety symptoms among pregnant individuals during the COVID-19 pandemic. *J Affect Disord*. 2020 Dec 1;277:5–13. <https://doi.org/10.1016/j.jad.2020.07.126>. Epub 2020 Aug 1. Erratum in: *J Affect Disord*. 2021 Jan 15;279:377–379. <https://doi.org/10.1016/j.jad.2020.10.012>
12. Courtemanche, R., et al.: Linking oscillations in cerebellar circuits. *Front Neural Circuits*. Jul 29;7:125 (2013). <https://doi.org/10.3389/fncir.2013.00125>
13. Chen, H., et al.: Theta synchronization between medial prefrontal cortex and cerebellum is associated with adaptive performance of associative learning behavior. *Sci Rep*. Feb 16;6:20960 (2016). <https://doi.org/10.1038/srep20960>
14. Sun, J.Y., Liu, F., Wang, H.X., et al.: Connectivity properties in the prefrontal cortex during working memory: a near-infrared spectroscopy study. *J Biomed Opt*. 2019 Mar;24(5):1–7. <https://doi.org/10.1117/1.JBO.24.5.051410>
15. Baek, S.J., Park, J.S., Kim, J., et al.: VTA-projecting cerebellar neurons mediate stress-dependent depression-like behaviors. *Elife*. 2022 Feb 14;11:e72981. <https://doi.org/10.7554/eLife.72981>
16. Moers-Hornikx, V.M., Sesia, T., Basar, K., et al.: Cerebellar nuclei are involved in impulsive behaviour. *Behav Brain Res*. 2009 Nov 5;203(2):256–63. <https://doi.org/10.1016/j.bbr.2009.05.011>. Epub 2009 May 18
17. Guo, W.B., Liu, F., Liu, J.R., et al.: Is there a cerebellar compensatory effort in first-episode, treatment-naive major depressive disorder at rest? *Prog Neuropsychopharmacol Biol Psychiatry*. 2013 Oct 1;46:13–8. <https://doi.org/10.1016/j.pnpbp.2013.06.009>. Epub 2013 Jun 23